21. Keenan, J. H., and F. G. Keyes, "Thermodynamic Properties of Steam," Wiley, New York (1936).
22. Keesom, W. H., A. Bijl, and J. F. A. A. Van Ireland, *Appl. Sci. Res. Section A*, **5**, 349 (1955).
23. Kobe, K. A., and Associates, "Thermochemistry of Petrochemicals," Bur. of Eng. Res., Univ. of Texas, Reprint No. 44, Austin, Texas.
24. Koppel, L. B., and J. M. Smith, *J. Chem. Eng. Data*, **5**, 437 (1960).
25. Landsbaum, E. M., W. S. Dodds, W. F. Stevens, B. J. Sollami, and L. F. Stutzman, *A.I.Ch.E. Journal*, **1**, 302 (1955).
26. Lydersen, A. L., R. A. Greenkorn, and O. A. Hougen, *Wisc. Univ. Eng. Exp. Sta. Rept. No. 4* (October, 1955).
27. Mage, D. T., M. L. Jones, Jr., D. L. Katz, and J. R. Roebuck, Paper presented at 48th National A.I.Ch.E. Meeting, Denver (August 26-29, 1962).
28. Matthews, C. S., and C. O. Hurd, *Trans. Am. Inst. Chem. Engrs.*, **42**, 55 (1946).
29. Mock, J. E., and J. M. Smith, *Ind. Eng. Chem.*, **42**, 2125 (1950).
30. Moore, D. A., Ph.D. thesis, Univ. of Mich., Ann Arbor, Michigan (1952).
31. O'brien, L. J., and W. J. Alford, *Ind. Eng. Chem.*, **43**, 506 (1951).
32. Organick, E. I., and W. R. Studhalter, *Chem. Eng. Progr.*, **44**, 847 (1948).
33. Opfell, J. B., W. G. Schlinger, and B. H. Sage, *Ind. Eng. Chem.*, **46**, 189 (1954).
34. Phillips Petroleum Company, unpublished data.
35. Prengle, H. W., L. R. Greenhaus, and R. York, *Chem. Eng. Progr.*, **44**, 863 (1948).
36. Reid, R. C., and J. M. Smith, *ibid.*, **47**, 415 (1951).
37. Rossini, F. D., K. S. Pitzer, R. L. Arnett, R. M. Braun, and G. C. Pimentel, "Selected Values of Physical and Thermodynamic Properties of Hydrocarbons and Related Compounds," API Project 44, Carnegie Press, Pittsburgh, Pennsylvania (1953).
38. Rynning, D. F., and C. O. Hurd, *Trans. Am. Inst. Chem. Engrs.*, **41**, 265 (1945).
39. Sage, B. H., and W. N. Lacey, *Ind. Eng. Chem.*, **30**, 873 (1938).
40. Schnaibal, H. C., and J. M. Smith, *Chem. Eng. Progr. Symposium Ser. No. 7*, **49**, 159 (1953).
41. Stevens, W. F., and George Thodos, *A.I.Ch.E. Journal*, **9**, 293 (1963).
42. Stuart, E. B., K. T. Yu, and J. Coull, *Chem. Eng. Progr.*, **46**, 311 (1950).
43. Sweigert, R. L., P. Weber, and R. L. Allen, *Ind. Eng. Chem.*, **38**, 185 (1946).
44. *U. S. Natl. Bureau Standards Circ. 142* (1923).
45. Weber, J. H., *A.I.Ch.E. Journal*, **1**, 210 (1955).
46. *Ibid.*, **2**, 514 (1956).
47. *Ibid.*, **5**, 17 (1959).
48. Williams, V. C., *Trans. Am. Inst. Chem. Engrs.*, **39**, 93 (1943).
49. Woolley, H. W., R. B. Scott, and F. G. Brickwedde, *J. Res. Natl. Bureau Standards*, **41**, 379 (1948).
50. York, R., and E. F. White, *Trans. Am. Inst. Chem. Engrs.*, **40**, 227 (1944).

Manuscript received June 30, 1964; revision received October 12, 1964; paper accepted November 2, 1964. Paper presented at A.I.Ch.E. Pittsburgh meeting.

Stability in Distributed Parameter Systems

NEAL R. AMUNDSON and LEE R. RAYMOND

University of Minnesota, Minneapolis, Minnesota

Three models of a catalyst particle are examined for existence of multiple steady states depending upon whether intraparticle heat conduction or diffusion is important. The particle with constant temperature but with intraparticle diffusion is examined in detail and a necessary and sufficient condition for the stability of the steady state is obtained. Calculations are made for a particle with both intraparticle diffusion and conduction and it is shown that there may be multiple steady states some of which are unstable to small perturbations.

In recent papers the problem of stability in systems in which chemical reactions are coupled with heat transfer and mass transfer has been treated in great detail. These systems all had the common characteristic that they were lumped constant systems in the sense that there were no distributed effects such as diffusion or conduction, and their mathematical formulation was as ordinary nonlinear differential equations for the transient state and algebraic equations in the steady state. There is little published literature on stability in distributed parameter systems, and it is the purpose of this paper to consider three mathematical models of essentially the same physical problem. The problem is related to the single catalyst particle but a gross idealization will be treated here. While this model may be grossly oversimplified, it is felt and hoped that it should give some insight into more complicated situations. For the purposes of this paper a catalyst particle in the form of a one-dimensional slab will be considered in which a simple first-order chemical reaction $A \rightarrow B$, irreversible, is assumed to take place. Heat may be generated or absorbed in the reaction, and hence the possibility of a temperature gradient within the particle exists. Three different models will be treated, one in more detail than the others. The lack of detail in the others is not to save space but rather because no rational approach other than that given here seems to be available at the moment.

The authors consider a slab catalyst particle of thickness l impervious at $x = 0$ and exposed to reactant at $x = l$. The three models may be briefly described as follows.

1. The temperature of the catalyst particle is uniform, and therefore conduction within it is neglected. The resistance to heat transfer is lumped at the particle surface at $x = l$. Knudsen diffusion of the reactant is the prevailing mode of mass transfer within the particle, and the Knudsen diffusion coefficient is assumed to be a constant. It is assumed that there is no mass transfer resistance at the particle surface, but relaxation of this restriction presents no difficulty. It is assumed in this model as well as the others that the chemical reaction can be expressed by means of a simple first-order rate law on the local partial pressure of reactant in the interstitial volume of the particle.

2. There is no resistance to mass transfer within the particle, and any resistance which may be present may be lumped at the surface $x = l$ and characterized by a mass transfer coefficient. Heat generated within the particle must be conducted to the surface through the particle, the heat carried by the reactants and products being neglected.

3. Neither conduction of heat nor diffusion of reactants is neglected, so that both forms of transport are distributed throughout the particle. Whereas in models 1 and 2 at least one of the two profiles in the particle was flat, in this model neither is. It is assumed that there is no transport resistance at the surface.

The model in which there is no distributed resistance has been treated earlier and in detail (*1, 3, 4*).

MODEL 1

With the usual nomenclature used in problems of this kind, the transient equations for the system are

$$D\frac{\partial^2 p}{\partial x^2} - \rho_s S_g k' p \exp\left(-\frac{E}{Rt}\right) = \sigma\frac{\partial p}{\partial \theta} \qquad (1)$$

$$h(t_o - t) + (-\Delta H)\,\rho_s S_g k' \exp\left(-\frac{E}{Rt}\right)\int_o^l p\,dx = l\,c_s\,\rho_s\frac{\partial t}{\partial \theta} \qquad (2)$$

$$p = p_o, \quad x = l, \quad \theta > 0 \qquad (3)$$

$$\frac{\partial p}{\partial x} = 0, \quad x = 0, \quad \theta > 0 \qquad (4)$$

$$p = p_i(x), \quad \theta = 0, \quad 0 < x < l \qquad (5)$$

$$t = t_i, \quad \theta = 0, \quad 0 < x < l \qquad (6)$$

The only term which needs attention in these equations is the second in Equation (2), where the rate at which heat is produced within the particle is the integrated rate throughout the particle, since the partial pressure depends upon position. The steady state equations follow directly from these to give

$$D\frac{\partial^2 p_s}{\partial x^2} - \rho_s S_g k' p_s \exp\left(-\frac{E}{Rt_s}\right) = 0 \qquad (7)$$

$$h(t_o - t_s) + (-\Delta H)\rho_s S_g k' \exp\left(-\frac{E}{Rt_s}\right)\int_o^l p_s\,dx = 0 \qquad (8)$$

$$p = p_o, \quad x = l, \quad \theta > 0 \qquad (3)$$

$$\frac{\partial p}{\partial x} = 0, \quad x = 0, \quad \theta > 0 \qquad (4)$$

This set of equations may be solved with ease, since Equation (7) is linear in p_s; although t_s is unknown, it is constant. The solution of Equation (7) subject to Equations (3) and (4) is

$$p_s(x) = p_o\frac{\cosh\frac{\Delta x}{l}}{\cosh\Delta} \qquad (9)$$

where

$$\Delta^2 = \rho_s S_g D^{-1} k' l^2 \exp\left(-\frac{E}{Rt_s}\right)$$

is a constant but still at this point unknown. Substitution of Equation (9) into Equation (8) gives

$$h(t_s - t_o) = (-\Delta H)\,p_o\frac{D}{l}\Delta\tanh\Delta \qquad (10)$$

The left-hand side is a linear function of t_s which represents the rate that heat can be released from the particle surface, while the right-hand side represents the rate at which heat is generated in the particle as a function of the particle temperature t_s. When the right-hand side is plotted as a function of t_s, a sigmoidal shaped curve as shown in Figure 1 is obtained whose intersections with the heat release curve gives the temperature of the steady state particle. It is clear that there may be some combinations of parameters which will produce multiple intersections and hence the possibility of multiple steady states for the particle exists. D_1, D_2, and D_3 are three lines for three different heat transfer coefficients.

A pertinent question then is whether all these states are stable or whether they can be realized, recognizing that every steady state is the result of a transient state. A steady state is said to be stable if when the particle is perturbed from that steady state it tends to return to the same state, and this is referred to as *local asymptotic stability*. Two approaches will be made here. In the first the transient equations will be linearized about the steady state and the equations examined to determine under what conditions small perturbations will approach zero asymptotically. In the second the nonlinear transient equations will be solved numerically to show in fact that the criteria developed in the first approach do in fact predict stability and instability. This latter work might appear to some to be redundant, but it is not clear, of course, that the linear equations are an adequate representation of the nonlinear equations in the small. For lumped parameter systems this is indeed a fact, as known from the well-known work of Lyapounov; however, analogous results for nonlinear partial differential equations are not known.

Equations (1) and (2) may be written in dimensionless form by defining new variables

$$v = \frac{t}{t_o}$$

$$u = \frac{p}{p_o}$$

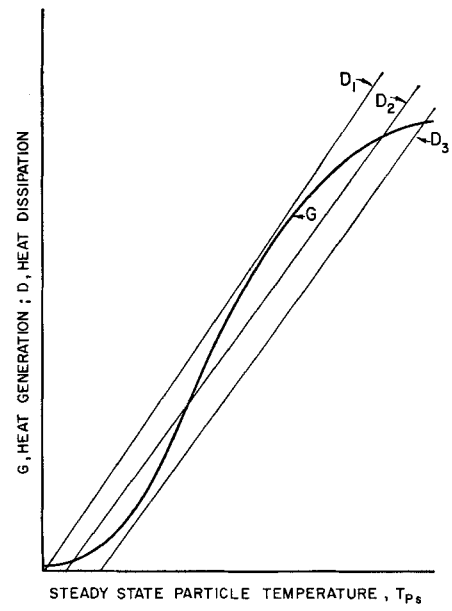

Fig. 1. Schematic diagram of heat release and heat generation curves corresponding to Equation (10).

$$r = \frac{x}{l}$$

$$\tau = \frac{D}{\sigma l^2}\theta$$

to give

$$H(1-v) + B\exp\left(-\frac{q}{v}\right)\int_0^1 u\,dr = \frac{\partial v}{\partial \tau} \quad (11)$$

$$\frac{\partial^2 u}{\partial r^2} - \alpha\, u \exp\left(-\frac{q}{v}\right) = \frac{\partial u}{\partial \tau} \quad (12)$$

with the conditions

$$u = 1, \quad r = 1, \quad \tau > 0 \quad (13)$$

$$\frac{\partial u}{\partial r} = 0, \quad r = 0, \quad \tau > 0 \quad (14)$$

$$u = u_i(r), \quad \tau = 0, \quad 0 < r < 1 \quad (15)$$

$$v = v_i \quad , \quad \tau = 0, \quad 0 < r < 1 \quad (16)$$

where $u = u(r, \tau)$ and $v = v(\tau)$. Also

$$H = \frac{h\, l\, \sigma}{c\rho_s\, D}$$

$$\beta = \frac{-\Delta H}{c_s}\,\frac{S_g\, k'\, l^2\, \sigma\, p_o}{t_o\, D}$$

$$\alpha = \frac{\rho_s\, S_g\, k'\, l^2}{D}, \quad \sigma = \frac{\gamma_v}{Rt_s}$$

$$q = \frac{E}{Rt_o}$$

Now consider the perturbations from the steady state, where the steady state partial pressure profile is given by

$$u_s(r) = \frac{\cosh \Delta r}{\cosh \Delta}$$

and the temperature is determined by Equation (10). The perturbations from the steady state are defined by

$$\xi = u - u_s$$

$$\eta = v - v_s$$

and the linearizations of Equations (11) and (12) are given by

$$-H\eta + \beta\left(-\frac{q}{v_s}\right)\int_0^1 \xi\,dr + \beta\left(\frac{q}{v_s}\right)\exp\left(-\frac{q}{v_s}\right)\eta\int_0^1 u_s\,dx = \frac{\partial \eta}{\partial \tau}$$

$$\frac{\partial^2 \xi}{\partial r^2} - \alpha \exp\left(-\frac{q}{v_s}\right)\xi - \alpha\, u_s \exp\left(-\frac{q}{v_s}\right)\left(\frac{q}{v_s^2}\right)\eta = \frac{\partial \xi}{\partial \tau}$$

These equations may be written in the form

$$-H\eta + c_{11}\int_0^1 \xi\,dr + c_{12}\,\eta = \frac{\partial \eta}{\partial \tau}$$

$$\frac{\partial^2 \xi}{\partial r^2} - c_{21}\,\xi - u_s\, c_{22}\,\eta = \frac{\partial \xi}{\partial \tau}$$

where c_{11}, c_{12}, c_{21}, and c_{22} are constants determined by the steady state temperature. In terms of the perturbations, Equations (13) through (16) become

$$\xi = 0, \quad r = 1, \quad \tau > 0$$

$$\frac{\partial \xi}{\partial r} = 0, \quad r = 0, \quad \tau > 0$$

$$\xi = \xi_i(r), \quad \tau = 0, \quad 0 < r < 1$$

$$\eta = \eta_i \quad , \quad \tau = 0, \quad 0 < r < 1$$

where the function $\xi_i(r)$ and the constant η_i are the initial perturbations from the steady state, which in the new variables is zero.

Now take the Laplace transforms of ξ and η as $\mathcal{L}(\xi) = U$ and $\mathcal{L}(\eta) = V$ with s as the transform variable and obtain

$$-HV + c_{11}\int_0^1 U\,dr + c_{12}\,V = s\,V - \eta_i \quad (17)$$

$$\frac{d^2U}{dr^2} - c_{21}\,U - u_s\, c_{22}\,V = s\,U - \xi_i \quad (18)$$

Let $\int_0^1 U\,dr = M$, a constant but unknown. Then the first equation may be solved for V to give

$$V = \frac{\eta_i + c_{11}\,M}{s + H - c_{12}}$$

which when substituted into Equation (18) gives

$$\frac{d^2U}{dr^2} - (\Delta^2 + s)\,U = -\xi_i(r) - \frac{u_s\, c_{22}\,(\eta_i + c_{11}\,M)}{s + H - c_{12}} \quad (19)$$

where it is to be noted that $\Delta^2 = c_{21}$. Equation (19) is of the form

$$\frac{d^2U}{dr^2} - \gamma^2\,U = f(r)$$

$$\gamma^2 = \Delta^2 + s$$

with boundary conditions

$$U = 0, \quad r = 0$$

$$\frac{dU}{dr} = 0, \quad r = 1$$

Its solution may be written in terms of the Green's function $G(r, \rho)$ as

$$U = \int_0^1 G(r, \rho)\, f(\rho)\, d\rho \quad (20)$$

where

$$G(r, \rho) = \begin{cases} \dfrac{\cosh \gamma\rho \sinh \gamma(r-1)}{\gamma \cosh \gamma}, & 0 < \rho < r \\ \dfrac{\cosh \gamma r \sinh \gamma(\rho - 1)}{\gamma \cosh \gamma}, & r < \rho < 1 \end{cases}$$

When the appropriate and extensive manipulations are made in Equation (20) by inserting the right-hand side of Equation (19) for $f(\rho)$, one obtains

$$U = -\int_0^1 \xi_i(\rho)\, G(r, \rho)\, d\rho + [\cosh \gamma r \cosh \Delta - \cosh \Delta r \cosh \gamma]\,\frac{c_{22}\,(\eta_i + c_{11}\,M)}{(s + H - c_{12})\,F}$$

where

$$F = (\gamma^2 - \Delta^2)\cosh \gamma \cosh \Delta$$

On the right-hand side M appears as the integral of U. Hence if this equation is integrated between zero and

one, an equation in M will be obtained which can be solved for M to give

$$M = \left\{ -\frac{E}{\gamma^2 \cosh\gamma} \int_0^1 (\cosh\gamma\rho - \cosh\gamma)\, \xi_i(\rho)\, d\rho + c_{22}\, \eta_i\, C(\gamma) \right\} D(\gamma)$$

where

$$D(\gamma)^{-1} = E - c_{11}\, c_{22}\, C(\gamma)$$

$$E = s + H - c_{12}$$

$$C(\gamma) = \frac{1}{\gamma^2 - \Delta^2}\left[\frac{\tanh\gamma}{\gamma} - \frac{\tanh\Delta}{\Delta} \right] \qquad (21)$$

U then may be written in the form

$$U = \frac{\eta_i\, \gamma^2 \cosh\gamma - c_{11} \int_0^1 (\cosh\gamma\rho - \cosh\gamma)\, \xi_i(\rho)\, d\rho}{\gamma^2 \cosh\gamma\, [E - c_{11}\, c_{22}\, C(\gamma)]} \qquad (22)$$

and V may be written as

$$V = \frac{\eta_i}{E - c_{11}\, c_{22}\, C(\gamma)} - \frac{c_{11} \int_0^1 (\cosh\gamma\rho - \cosh\gamma)\, \xi_i(\rho)\, d\rho}{\gamma^2 \cosh\gamma\, [E - c_{11}\, c_{22}\, C(\gamma)]} \qquad (23)$$

Now Equations (22) and (23) are the Laplace transforms of the response to arbitrary but small perturbations in the partial pressure and the temperature. However, the authors' interest is only in whether the perturbations approach zero asymptotically with the time. It is evident after some examination that one need be concerned only with the nature of the zeroes of

$$\gamma^2 \cosh\gamma$$

$$E - c_{11}\, c_{22}\, C(\gamma)$$

considered as functions of s, for the only singularities of U and V are poles. If all the zeroes have negative real parts, then one can be assured that the perturbations will damp to zero. If there is a zero with positive real part, the perturbation will grow. It is apparent that the zeroes of $\gamma^2 \cosh\gamma$ considered as functions of s will have negative real parts, and they are in fact

$$s = -\Delta^2$$

and

$$s = -\Delta^2 - \frac{(2n+1)^2\pi^2}{4},\quad n = 0, 1, 2, 3, \ldots$$

The function $E - c_{11}\, c_{22}\, C(\gamma) = 0$ may be written in the form

$$s^2 + s(H - c_{12}) + c_{11}\, c_{22}\frac{\tanh\Delta}{\Delta} = c_{11}\, c_{22}\frac{\tanh\gamma}{\gamma}$$

or

$$s^2 + bs + c = k\frac{\tanh\Delta}{\gamma},\quad c > 0,\ k > 0 \qquad (24)$$

after multiplying through by $\gamma^2 - \Delta^2$.

The analysis necessary to determine the character of the values of s which satisfy this equation are sufficiently novel to present it in some detail, although it is somewhat lengthy. The analysis depends upon two theorems from complex variables, Rouche's theorem (2) and the principle of the argument (2). By means of Rouche's theorem one can make an accounting of all of the roots, and by the principle of the argument, one can determine whether any roots lie in a particular portion of the complex plane.

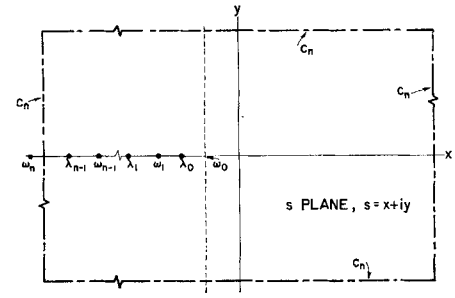

Fig. 2. Schematic diagram showing zeroes and poles for the application of Rouche's theorem.

Rouche's Theorem

If $f(z)$ and $g(z)$ are two functions analytic within and on a closed contour C on which $f(z)$ does not vanish and also $|f(z)| > |g(z)|$ on C, then $f(z)$ and $f(z) + g(z)$ have the same number of zeroes within C.

Some of the details will be omitted. Consider a square in the complex s plane with sides parallel to the real and imaginary axes with the center of the square at the origin.

The poles of $\dfrac{\tanh\gamma}{\gamma}$ occur at

$$\lambda_n = -\Delta^2 - \left(n + \frac{1}{2}\right)^2\pi^2,\quad n = 0, 1, 2, \ldots$$

while the zeroes are at

$$\omega_n = -\Delta^2 - n^2\pi^2,\quad n = 1, 2, \ldots$$

and the poles and zeroes interlace each other. Choose the vertical sides of the square at $s = \pm\Delta^2 \pm \left(n - \dfrac{1}{4}\right)^2\pi^2$ so that these lines avoid the zeroes and poles. A schematic diagram is shown in Figure 2. Let the square contour be denoted by C_n. For large n it may be shown with ease that $\dfrac{\tanh\gamma}{\gamma}$ is analytic and bounded on C_n and, in fact, approaches zero as $n \to \infty$ on C_n. Since $s^2 + bs + c$ is analytic in the whole plane and behaves like s^2 for $|s|$ large

$$|s^2 + bs + c| > \left| k\frac{\tanh\gamma}{\gamma} \right|$$

on C_n and for n large, and therefore

$$|s^2 + bs + c|\ |\cosh\gamma| > k\left|\frac{\sinh\gamma}{\gamma}\right|$$

on C_n for n large. Therefore since the functions $(s^2 + bs + c)\cosh\gamma$ and $k\dfrac{\sinh\gamma}{\gamma}$ are analytic inside C_n, by

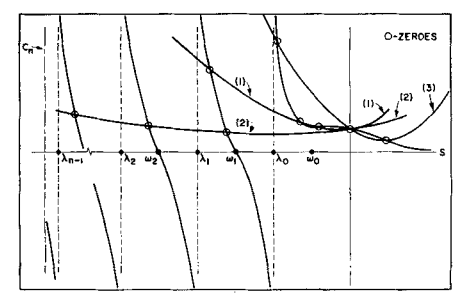

Fig. 3. Schematic diagram showing real values of s satisfying Equation (24).

Rouche's theorem the function $(s^2 + bs + c)\cosh\gamma$ has the same number of zeroes inside C_n as

$$(s^2 + bs + c)(\cosh\gamma) - k\frac{\sinh\gamma}{\gamma}$$

does. The quantity $s^2 + bs + c$ has 2 zeroes inside C_n and $\cosh\gamma$ has n at $\lambda_0, \lambda_1, \lambda_2, \ldots, \lambda_{n-1}$. Hence

$$s^2 + bs + c - k\frac{\tanh\gamma}{\gamma} = 0$$

has $(n + 2)$ zeroes in C_n. This function will have some real zeroes, and inside C_n these may be counted. Figure 3 shows a schematic diagram of

$$\frac{\tanh\gamma}{\gamma} \text{ and } s^2 + bs + c$$

plotted against real s. Curves (1), (2), and (3)are three different positions (among others) for the quadratic function, and these show that there will always be at least n real intersections while for curves (1) and (3) there are $n + 2$ real intersections. Curve (3) shows that there is one positive real intersection. Curve (2) shows only n intersections so that there must be two more and these will be complex. Therefore from Rouche's theorem one is able to show that there will always be n real and negative zeroes, and hence there can only be two other zeroes. If there is one positive zero, then there must be $(n + 1)$ real negative zeroes. Figure 4 is a schematic diagram similar to Figure 3 but with more attention paid to the topology as b varies. Note that in Figure 4 only the branch of $\frac{\tanh\gamma}{\gamma}$ which occurs furthest to the right is shown along with $s^2 + bs + c$. For $b = 0$ from Figures 3 and 4 all of the zeroes of

$$s^2 + bs + k\frac{\tanh\Delta}{\Delta} - k\frac{\tanh\gamma}{\gamma} = 0$$

are accounted for since all are real. The same is true for $b < 0$. It is also clear that for values of b increasing from 0 the two intersections in the left half plane will move together and eventually coalesce at P. For values of b greater than this critical value the number of real intersections will decrease by two, and hence for $b > b_c > 0$ there will be two complex zeroes. For values of $b < 0$

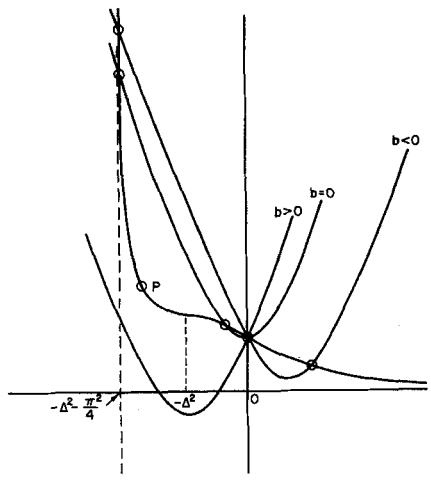

Fig. 4. Detailed schematic diagram of Figure 3 showing intersections for various values of b for rightmost branch.

$$b < k\left[\frac{d}{ds}\left(\frac{\tanh\gamma}{\gamma}\right)\right]_{s=0}$$

that is such that the slope of the quadratic is less than the slope of $\frac{\tanh\gamma}{\gamma}$. At $s = 0$ there will be no positive real intersections. The slope restriction above may be written in the form

$$b \geqq -\frac{k}{2\Delta^3}(\tanh\Delta - \Delta\,\mathrm{sech}^2\Delta)$$

This is certainly a necessary and sufficient condition that there be no positive real zeroes. It would also be a necessary and sufficient condition for stability if it can also be shown that the complex zeroes for $b > 0$ have negative real parts. The authors will now show that for $b > 0$ there are no zeroes in the right half plane, and hence the necessary and sufficient condition for stability is the restriction above which when combined with the definition of b gives

$$H > \frac{1}{2}\frac{\beta}{\alpha}\frac{q}{v_s^2}\Delta(\tanh\Delta + \Delta\,\mathrm{sech}^2\Delta)$$

(The equality sign must be investigated separately later.)

PRINCIPLE OF THE ARGUMENT

If $f(z)$ is analytic inside and on a closed contour C and is not zero on the contour, then if N is the number of zeroes of $f(z)$ inside C, the change in the value of the argument of $f(z)$ when C is traversed once is $2\pi N$ or

$$N = \frac{\Delta_c\, arg\, f(z)}{\pi}$$

where $\Delta_c\, arg\, f(z)$ is the change in the argument as C is traversed once in the z plane. The function is written as

$$\phi = s^2 + bs + c - k\frac{\tanh\sqrt{\Delta^2 + s}}{\sqrt{\Delta^2 + s}}$$

In the right half plane of s, ϕ is analytic, and one seeks to determine whether there are any zeroes there. Make the change of variable

$$w = \sqrt{\Delta^2 + s}, \quad s = w^2 - \Delta^2$$

$$\phi = (w^2 - \Delta^2)^2 + b(w^2 - \Delta^2) + c - k\frac{\tanh w}{w}$$

Now the mapping $w = \sqrt{\Delta^2 + s}$ maps the right half plane of s into the interior of the right branch of an hyperbola as in Figure 5, since if

$$w = u + iv$$

then

$$u^2 - v^2 = \Delta^2 + x$$

$$2uv = y$$

The imaginary axis $x = 0$ maps into $u^2 - v^2 = \Delta^2$ and any point for which $x > 0$ maps into a point interior to the branch of the right hyperbola. As the axis of imaginaries is traversed from $+\infty$ to $-\infty$, the hyperbola is traversed from $u = \infty$, $v = \infty$ to $u = \Delta$, $v = 0$ to $u = \infty$, $v = -\infty$. If ϕ has a zero in the right half plane of s, it will map into the interior of the hyperbola as a zero in terms of w. Since ϕ is an even function of w, a zero in the interior of the right hyperbola will have an image zero in the left hyperbola symmetric with respect to the origin. If there is a pure imaginary zero in the s plane, it will appear on the hyperbola in the w plane.

The function ϕ may be written as

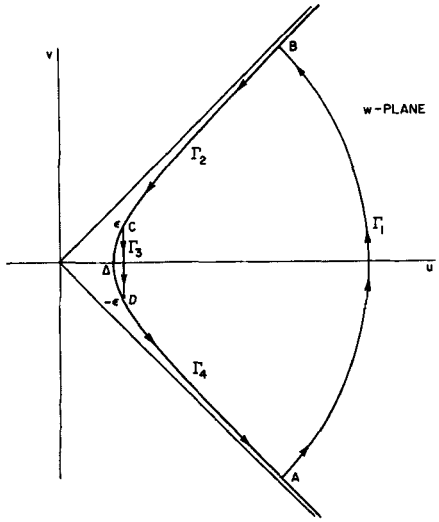

Fig. 5. Closed contour Γ_1 Γ_2 Γ_3 Γ_4 used in the principle of the argument.

$$\phi(w) = \Gamma + i\Omega$$

where

$$\Gamma = (u^2 - v^2 - \Delta^2)^2 - 4u^2v^2 + b(u^2 - v^2 - \Delta^2) + c - k\,H(u,v) \quad (24)$$

$$\Omega = 4uv(u^2 - v^2 - \Delta^2) + 2buv + k\,G(u,v) \quad (25)$$

$$H(u,v) = \frac{u \tanh u \sec^2 v + v \tan v \operatorname{sech}^2 u}{(1 + \tanh^2 u \tan^2 v)(u^2 + v^2)}$$

$$G(u,v) = \frac{v \tanh u \sec^2 v - u \operatorname{sech}^2 u \tan v}{(1 + \tanh^2 u \tan^2 v)(u^2 + v^2)}$$

It may be shown with ease that G and H are bounded for all u and v and that

$$H(u,v) > 0 \text{ for all } u \text{ and } v$$

$$H(u,0) = \frac{\tanh u}{u}$$

$$G(u,0) = 0$$

$$G(u,v) > 0, \quad u > 0, \quad v > 0$$

$$G(u,v) < 0, \quad u > 0, \quad v < 0$$

Now consider how the argument of w changes as one traverses a path consisting of the circular segment Γ_1 from A to B, the section of the hyperbola Γ_2 from B to C, the vertical straight line Γ_3 from C to D, and the hyperbolic segment Γ_4 from D to A. The straight line segment is used in order to avoid the zero in ϕ at $u = \Delta$, $v = 0$ on the hyperbola. Suppose the coordinates of C are $v = \epsilon$, $u = \sqrt{\Delta^2 + \epsilon^2}$, where ϵ is small.

Now

$$arg\,\phi = \tan^{-1}\frac{\Omega}{\Gamma} \quad (26)$$

and on the hyperbola

$$arg\,\phi = \tan^{-1}\frac{2buv + k\,G(u,v)}{-4u^2v^2 + c - k\,H(u,v)} \quad (27)$$

For $v = \epsilon$ it may be shown that on the hyperbola

$$arg\,\phi = \tan^{-1}\frac{K_1\epsilon + H.O.T.}{-K_2\epsilon^2 + H.O.T.} \quad (28)$$

and for $v = -\epsilon$ on the hyperbola

$$arg\,\phi = \tan^{-1}\frac{-K_1\epsilon + H.O.T.}{-K_2\epsilon^2 + H.O.T.} \quad (29)$$

where

$$K_1 = 2\Delta\left[H - \frac{1}{2}\frac{\beta}{\alpha}\frac{q}{v_s^2}\Delta(\tanh\Delta + \Delta\operatorname{sech}^2\Delta)\right]$$

$$K_2 = \Delta^2\left[4 - \frac{\beta}{\alpha}\frac{q}{v_s^2}\left(\Delta\tanh^3\Delta + \frac{3}{2}\tanh^2\Delta + \left(\frac{3}{2\Delta} - \Delta\right)\tanh\Delta - \frac{3}{2}\right)\right]$$

It may be shown that the quantity in the parenthesis in K_2 is always a positive function, zero only for $\Delta \to o$ and $\Delta \to \infty$. If $b > 0$, $K_1 > 0$. For an endothermic reaction $K_2 > 0$ and $K_1 > 0$. Now consider how the argument changes over the whole path Γ_1 Γ_2 Γ_3 Γ_4. For an exothermic reaction K_2 could be negative.

On Γ_1. ϕ may be written

$$\phi = w^4\left[1 + \frac{b - 2\Delta^2}{w^2} + \frac{\Delta^4 - b\Delta^2 + c}{w^4} - k\frac{\tanh w}{w^5}\right]$$

and

$$arg\,\phi = arg\,w^4 + arg\left[1 + 0\left(\frac{1}{R^2}\right)\right]$$

$$= arg\,(R^4 e^{4i\theta}) + arg\left[1 + 0\left(\frac{1}{R^2}\right)\right]$$

Hence as $arg\,w$ changes from $-\frac{\pi}{4} + \eta$ to $\frac{\pi}{4} - \eta$, $arg\,\phi$ changes from $-\pi + 4\eta$ to $\pi - 4\eta$ for η small, $\Delta\,arg\,\phi$ is $2\pi - 8\eta$, or in the limit as $R \to \infty$, $\Delta\,arg\,\phi$ on Γ_1 is 2π. Consider first the case for $K_2 > 0$.

On Γ_2. From Equation (27) for u and v very large and positive because of the boundedness of G and H, it follows that $arg\,\phi = \pi - \eta$ for $b > 0$. As Γ_2 is traversed, the numerator decreases but remains positive. The denominator is initially negative, and ultimately as C is approached, Γ_2 is negative but becomes very small. Hence at C $arg\,\phi$ is $\frac{\pi}{2} + \eta$, so that $\Delta\,arg\,\phi$ on Γ_2 is $-\frac{\pi}{2} + 2\eta$. If it should happen that the denominator in Equation (27) should vanish as Γ_2 is traversed from B to C, then the argument will change, but since the fraction itself cannot pass through zero, the net change in the argument must be as described. In particular, if the denominator vanishes once since it is originally negative, it must pass through zero and becomes positive as C is approached. But this is impossible since at C the denominator is negative. Hence if it vanishes once it must vanish again in order that the denominator may become negative. But the net change in the argument as the denominator passes through an even number of zeroes must be zero since the fraction itself does not pass through zero. The argument of ϕ in this case must oscillate about $\frac{\pi}{2}$.

On Γ_3. At C $arg\,\phi = \frac{\pi}{2} + \eta$, the denominator in Equation (28) is negative, and the numerator is positive. As one approaches the real axis on Γ_3, from Equations (24) and (25) it becomes apparent that the numerator in Equation (26), Ω, is always positive and approaches zero at the axis. The denominator on the other hand is negative at C becomes more positive and at the real axis is positive, for $b > 0$ and hence must pass through zero. Therefore $arg\,\phi$ must pass from $\frac{\pi}{2} + \eta$ to $\frac{\pi}{2}$ to $\frac{\pi}{2} - \eta$ to 0. The net

change in $arg\,\phi$ is thus $-\frac{\pi}{2}-\eta$ as Γ_3 from C to the axis is traversed. As Γ_3 is traversed below the axis, the argument of ϕ will change from 0 to $-\frac{\pi}{2}-\eta$ by the same argument, and so $\Delta\, arg\,\phi$ is $-\pi$ on Γ_3.

On Γ_4. The same argument as that used on Γ_2 will show that on Γ_4 $\Delta\, arg\,\phi = -\frac{\pi}{2} + 2\eta$.

If one now lets the straight line segment Γ_3 approach the point $u = \Delta$, $v = 0$ and also lets the radius of the circular portion Γ_1 become infinite, then it is apparent that the net change in the argument is the sum of the net changes on each of the separate segments; for $b > 0$ this is zero. Thus there can be no zeroes with positive real parts if $b > 0$ and $K_2 > 0$. A similar argument will show that if $b > 0$ but $K_2 < 0$ the same result obtains. Hence the necessary and sufficient condition for stability is the same as the necessary and sufficient condition that there be no positive real zeroes.

If one considers the slope of the heat generation curve and heat rejection curve of Figure 1 at the point of intersection, then if heat is to be rejected faster than it is generated for a small perturbation the slope of the rejection curve must be greater than the slope of the generation curve or

$$h > (-\Delta H)\, p_o \frac{D}{l}\left[\frac{d}{dt}(\Delta \tanh \Delta)\right]_{t=t_s}$$

This may be put into the form

$$H > \frac{\beta}{\alpha}\,\frac{\Delta}{2}\,\frac{q}{v_o^2}\,[\tanh \Delta + \Delta \operatorname{sech}^2 \Delta]$$

which is the same as the condition derived above for stability.

Two final points need clearing up. The first involves the existence of pure imaginary zeroes. This is clearly impossible since the function Ω on the hyperbola does not vanish except at $v = 0$, $u = \Delta$ which is the origin in the s plane. The second point involves the possibility of $s = 0$ being a double zero when the parabola is tangent to the curve $\frac{\tanh \gamma}{\gamma}$ at $s = 0$. In Equations (22) and (23) there is in fact a factor of $\gamma^2 - \Delta^2$ in the numerator since $C(\gamma)$ in Equation (21) has such a factor in the denominator. Thus at $s = 0$ the denominator really has only a single zero in Equations (22) and (23). Since this zero must be avoided, it follows that the equality in the condition

$$H > \frac{1}{2}\,\frac{\beta}{\alpha}\,\frac{q}{v_s}\,\Delta\,(\tanh \Delta + \Delta \operatorname{sech} \Delta^2)$$

must be avoided for stability. If the inequality is not satisfied, the particle is unstable.

In order to illustrate the behavior of this model a numerical example will be illustrated. This example was chosen to illustrate a possible behavior for the model. The data used in the example are given in Table 1. In this example it is necessary to compute and plot the heat generation and heat rejection curves as given by Equation (10) and Figure 1 in order to determine the number of steady states. Once this has been done the criterion for stability may be applied to the steady state. Computations have also been made on the full nonlinear equations for small and large perturbations. These computations are long and require a large amount of computer time and in themselves involve little that is novel, so that the method used will not be described in detail except to state that considerable effort was expended in choosing appropriate time and space increments for the finite difference approximations to the differential equations and auxiliary conditions, Equations (11) to (16).

TABLE 1. DATA FOR ILLUSTRATIVE PROBLEM—MODEL 1

ΔH	$= -30{,}000$ cal./g. mole A
M_A	$= 36$ g./g. mole A
t_p	$= 350$°K.
p_p	$= 0.10$ atm.
E	$= 13{,}000$ cal./g. mole A
k	$= 7.80 \times 10^{-3}$ g. mole A/sq. cm. atm. sec.
l	$= 1.0$ cm.
γ	$= 0.50$
$\bar{r}$	$= 100$Å
ρ_s	$= 1.2$ g./cc.
c_s	$= 0.25$ cal./g. °K.
D	$= 2.22 \times 10^{-7}$ g. mole/cm. atm. sec.
h	$= 10^{-3}$ cal./sq. cm. sec. °K.
$\rho_s S_g$	$= 10^6$ sq. cm./g.

In this example there are three steady state temperatures at 367.1°, 475.0°, and 12,800°K., and the lower portion of the rejection-generation curves is shown in Figure 6. The upper intersection while realizable mathematically makes no sense physically. The condition $b > 0$ is met at the upper and lower state but not at the intermediate state. Transient calculations are shown in Figures 7 and 8 for the lower and intermediate steady states, respectively. Figure 7 was calculated for a 5% negative partial pressure perturbation from the steady state. The state is clearly stable to small perturbations. Figure 8 was calculated for a 5% positive partial pressure perturbation and shows that this state is unstable. Other perturbations produce a similar result. No computations are made for the upper steady state.

MODEL 2

This model is essentially the converse of Model 1 and assumes that heat transport is distributed and mass transfer is lumped. With these assumptions and some others the equations describing a slab catalyst may be put in the form

$$\lambda \frac{\partial^2 t}{\partial x^2} + \rho_s S_g (-\Delta H)\, p\, k' \exp\left(-\frac{E}{Rt}\right) = c_s \rho_s \frac{\partial t}{\partial \theta} \tag{33}$$

$$k_g(p_o - p) - k' p \rho_s S_g \int_o^t \exp\left(-\frac{E}{Rt}\right) dx = \frac{\partial p}{\partial \theta} \tag{34}$$

$$\frac{\partial t}{\partial x} = 0, \quad x = 0, \quad \theta > 0 \tag{35}$$

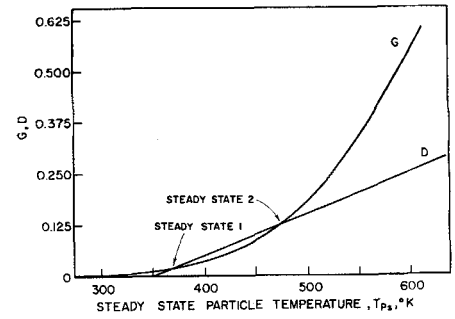

Fig. 6. Plot of lower portion of heat generation and heat rejection curves for numerical example in Model 1.

$$t = t_o, \quad x = l, \quad \theta > 0 \tag{36}$$
$$t = t_i(x), \quad \theta = 0, \quad 0 < x < l$$
$$p = p_i, \quad \theta = 0, \quad 0 < x < l$$

These can be put into dimensionless form to give

$$\frac{\partial^2 v}{\partial r^2} + \omega u \exp\left(-\frac{q}{v}\right) = \frac{\partial v}{\partial \tau'} \tag{37}$$

$$K(1-u) - \mu u \int_0^1 \exp\left(-\frac{q}{v}\right) dr = \frac{\partial u}{\partial \tau'} \tag{38}$$

$$\frac{\partial v}{\partial r} = 0, \quad r = 0, \quad \tau' > 0 \tag{39}$$

$$v = 1, \quad r = 1, \quad \tau' > 0 \tag{40}$$

$$u = u_i, \quad \tau' = 0, \quad 0 < r < 1$$
$$v = v_i(r), \quad \tau' = 0, \quad 0 < r < 1$$

and new dimensionless variables are

$$\tau' = \frac{\lambda \theta}{c_s \rho_s l^2}$$

$$\omega = \frac{\rho_s S_g (-\Delta H) p_o k' l^2}{\lambda t_o}$$

$$\mu = \frac{k' l^2 \rho_s^2 S_g c_s}{\sigma \lambda}$$

$$K = \frac{k_g c_s \rho_s l^2}{\sigma \lambda}$$

In this model the authors will only show how the steady state calculations may be approached. It is not clear how a detailed analysis of this problem should be pursued. The following two equations for the steady state partial pressure may be derived after some manipulation:

$$u_s = \int_1^{v_{sc}} \frac{dv_s}{\sqrt{2\omega \int_v^{v_{sc}} \exp\left(-\frac{q}{v_s}\right) dv_s}} \tag{41}$$

$$\sqrt{u_s} = \frac{2K}{\mu f(v_{sc}) + \sqrt{\mu f(v_{sc})^2 + 4K^2}} \tag{42}$$

where

$$f(v_{sc}) = \int_1^{v_{sc}} \frac{\exp\left(-\frac{q}{v_s}\right) dv_s}{\sqrt{2\omega \int_v^{v_{sc}} \exp\left(-\frac{q}{v_s}\right) dv_s}}$$

The simultaneous satisfaction of Equations (41) and (42) will then give the temperature at the center of the catalyst pellet, and the partial pressure in the pellet then follows from Equation (42). This model will not be carried through any further.

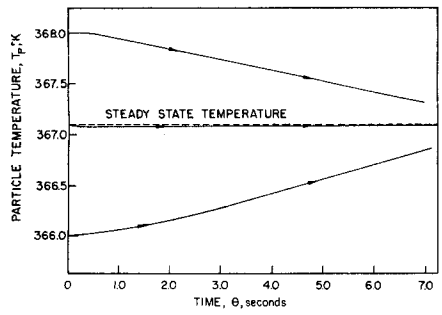

Fig. 7. Transient calculations for perturbations about lower stable steady state shown in Figure 6.

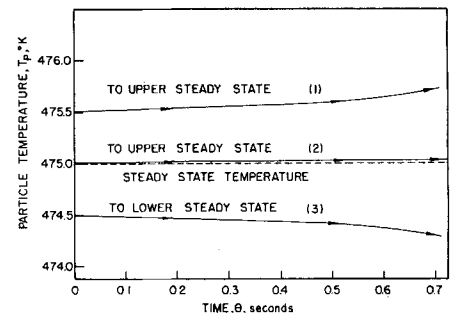

Fig. 8. Transient calculations for intermediate unstable steady state for numerical example in Model 1.

MODEL 3

This model is by far the most complex and one for which theoretical results are almost unavailable since the stability analysis requires mathematics which have not been done and which according to experts will not be soon in coming. However, some results may be obtained. In this model it is assumed that both heat transfer and mass transfer are distributed so that the general equations describing the system for a simple reaction are

$$D \frac{\partial^2 p}{\partial x^2} - \rho_s S_g k' p \exp\left(-\frac{E}{Rt}\right) = \sigma \frac{\partial p}{\partial \theta} \tag{43}$$

$$\lambda(1-\gamma) \frac{\partial^2 t}{\partial x^2} + \rho_s S_g k' (-\Delta H) p \exp\left(-\frac{E}{Rt}\right) = c_s \rho_s \frac{\partial t}{\partial \theta} \tag{44}$$

$$\frac{\partial p}{\partial x} = 0, \quad x = 0, \quad \theta > 0 \tag{45}$$

$$\frac{\partial t}{\partial x} = 0, \quad x = 0, \quad \theta > 0 \tag{46}$$

$$p = p_o, \quad x = l, \quad \theta > 0 \tag{47}$$

$$t = t_o, \quad x = 1, \quad \theta > 0 \tag{48}$$

$$p = p_i(x), \quad \theta = 0, \quad 0 < x < l$$
$$t = t_i(x), \quad \theta = 0, \quad 0 < x < l$$

The steady state equations are

$$D \frac{d^2 p_s}{dx^2} - \rho_s S_g k' p_s \exp\left(-\frac{E}{Rt_s}\right) = 0$$

$$\lambda(1-\gamma) \frac{d^2 t_s}{dx^2} + \rho_s S_g k' (-\Delta H) p_s \exp\left(-\frac{E}{Rt_s}\right) = 0$$

These can be put in the dimensionless form on letting $z = \frac{p_s}{p_o}$, $y = \frac{t_s}{t_o}$

$$\frac{d^2 z}{dr^2} - B z \exp\left(-\frac{q}{y}\right) = 0 \tag{49}$$

$$\frac{d^2 y}{dr^2} + A z \exp\left(-\frac{q}{y}\right) = 0 \tag{50}$$

with the constants

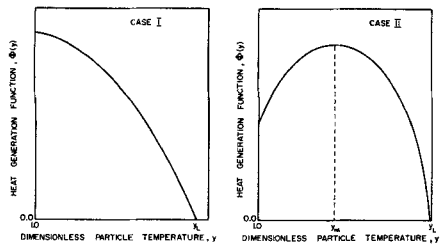

Fig. 9. Schematic diagram of heat generation functions.

$$B = \frac{\rho_s S_g k' l^2}{D}$$

$$A = \frac{\rho_s S_g k' l^2 p_o}{t_o \lambda (1-\gamma)} (-\Delta H)$$

From Equations (49) and (50) by elimination and integration

$$y = 1 + \frac{A}{B}(1-z)$$

A limiting temperature y_L may be defined for $z = 0$

$$y_L = 1 + \frac{A}{B}$$

so that

$$y = y_L - \frac{A}{B} z$$

Equation (50) may then be put into the form

$$\frac{d^2y}{dr^2} + B(y_L - y) \exp\left(-\frac{q}{y}\right) = 0$$

This may be integrated once to give

$$\frac{dy}{dr} = -\sqrt{2B \int_y^{y_c} (y_L - y) \exp\left(-\frac{q}{y}\right) dy}$$

and letting

$$\phi(y) = B(y_L - y) \exp\left(-\frac{q}{y}\right)$$

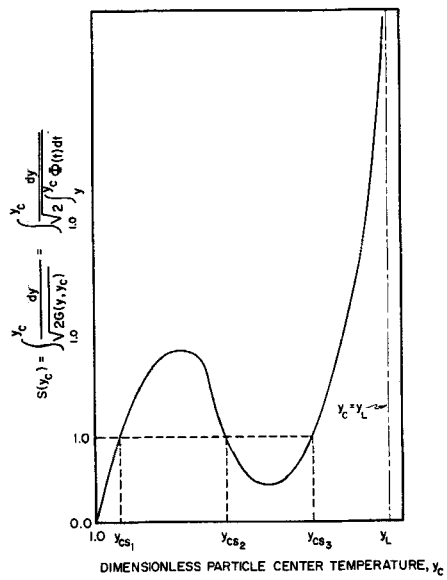

Fig. 10. Schematic diagram of $S(y_c)$ vs. y_c. Case II.

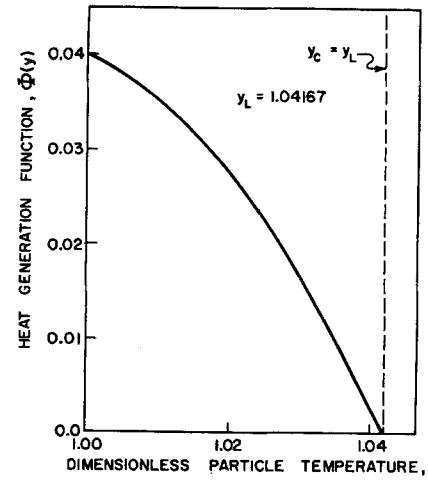

Fig. 11. Heat generation curve for Problem 1, Model 3. Single steady state.

a second integration gives over the whole particle

$$1 = S(y_c) = \int_1^{y_c} \frac{dy}{\sqrt{2\int_y^{y_c} \phi(t)\,dt}} \qquad (51)$$

Equation (51) is an equation for the determination of y_c, and the number of y_c's which will satisfy the equation determines the number of steady states the problem may have. The integral in Equation (51) is an improper integral, but a simple analysis will show that it exists. The remainder of the work on this model will revolve around a discussion of Equation (51), some examples to illustrate what can happen, and some transient calculations on these examples.

The function $\phi(y)$ will be referred to as the *heat generation function* and its integral is defined as

$$G(y, y_c) = \int_y^{y_c} \phi(t)\,dt$$

The heat generation function has a maximum at

$$y_m = \frac{-q + \sqrt{q^2 + 4q\,y_L}}{2}$$

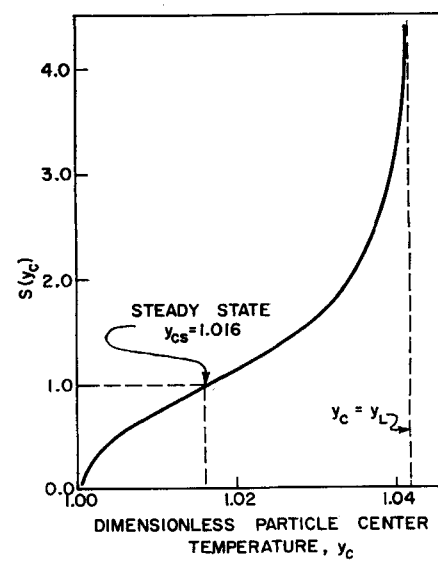

Fig. 12. $S(y_c)$ for Problem 1, Model 3. Single steady state.

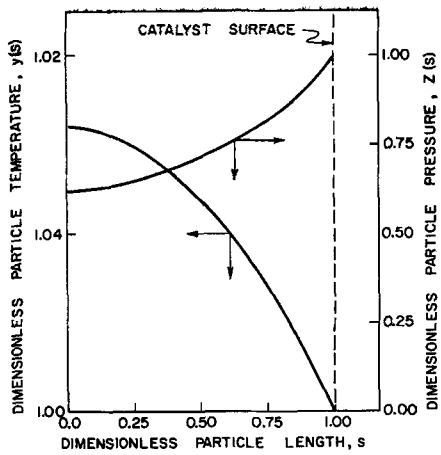

Fig. 13. Dimensionless temperature and partial pressure profiles for Problem 1, Model 3.

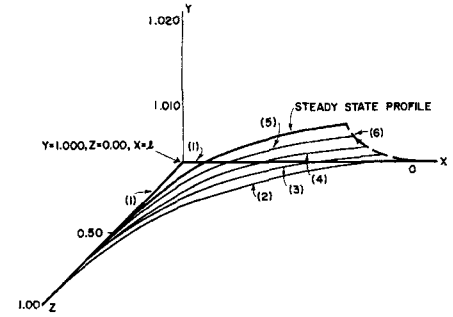

Fig. 15. Phase space plot showing transient response surface for Problem 1, Model 3.

as may be directly computed. Furthermore $\phi(y_L) = 0$. $\phi(y)$ when plotted against y has the appearance of either Case I or Case II in Figure 9 depending upon whether $y_m < 1$ if $t_m > 1$. The function $S(y_c)$ may be plotted vs. y_c, and in general curves of the type shown in Figure 10 are obtained. In Figure 10 it is clear that three steady states are shown to be possible, although if $S(1)$ were large enough there would be one steady state. In most cases the curve of $S(y_c)$ vs. y_c is monotonically increasing, and only one state is possible. The quantities which can vary substantially are the activation energy, the heat of reaction, and the frequency factor.

Activation energy: Changes in E do not alter y_L but do change the position of y_m and the qualitative characteristics of $\phi(y)$. Computations show that the possibility of multiple states becomes more likely with higher activation energies. For $E = 0$, there is always only one state.

Heat of reaction: Changes in ΔH alter both y_L and y_m, and the possibility of multiple steady states becomes greater when $(-\Delta H)$ is large. For $\Delta H > 0$ there is always only one state.

Frequency factor: Changes in k do not change y_L or y_m, and since $S(y_c)$ is directly proportional to $k^{-1/2}$ the net effect of changes in k is to shift the line $S(y_c) = 1$ up or down.

From Figure 10 it is apparent that there can only be multiple states when the derivative $S(y_c)$ is negative at some point. Now one can compute the derivative of $S(y_c)$ with respect to y_c as

$$S'(y_c) = \frac{\phi(y_c)}{\phi(1)\sqrt{G(1, y_c)}} - \phi(y_c) \int_1^{y_c} \frac{\phi'(y)\, dy}{\phi(y)^2 \sqrt{2G(y, y_c)}}$$

and if the derivative is to be negative then

$$\int_1^{y_c} \frac{\phi'(y)\, dy}{\phi(y)^2 \sqrt{2G(y, y_c)}} > \frac{1}{\phi(1)\sqrt{G(1, y_c)}}$$

for some y_c. This is a necessary condition for the possibility of multiple steady states but its use is more difficult than computing $S(y_c)$ itself. In order that $\phi(y)$ have a maximum, $1 < y_m < y_L$, obviously. It can be shown that multiple steady states can occur only in the case in which the heat generation function has a maximum as in Case II, Figure 9. But as the examples below will show, this is not a sufficient condition. It would be desirable to make some more definitive statements about when multiple states oc-

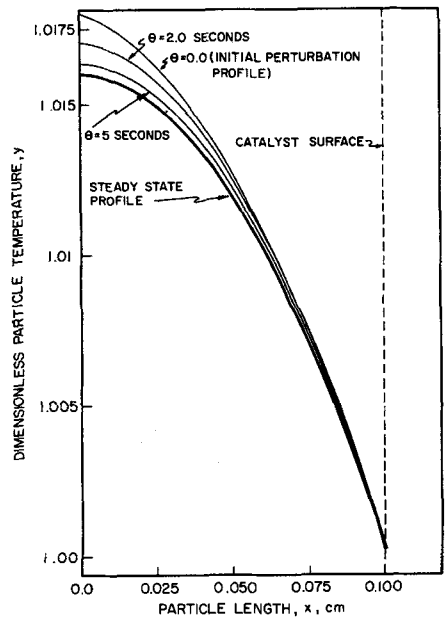

Fig. 14. Transient dimensionless particle temperature profiles, Problem 1, Model 3.

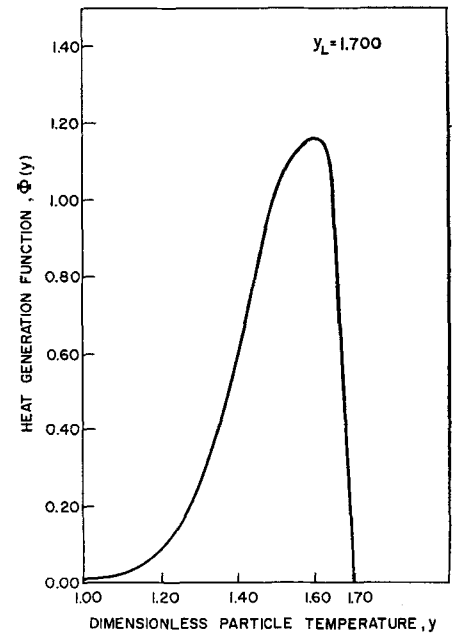

Fig. 16. Heat generation function for Problem 2, Model 3.

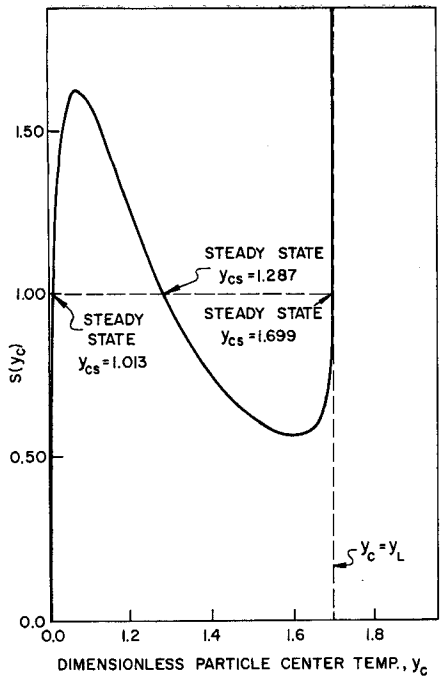

Fig. 17. $S(y_c)$ curve for Problem 2, Model 3, showing three steady states.

cur and, if they occur, which are stable or unstable, but, unfortunately, this is not possible.

The problem of finding the temperature and partial pressure profiles is now simpler than it might have been, for one can now replace the system

$$\frac{d^2y}{dr^2} + \phi(y) = 0$$

$$y'(0) = 0, \quad r = 0$$

$$y(1) = 1, \quad r = 1$$

by

$$\frac{d^2y}{dr^2} + \phi(y) = 0$$

$$y(0) = y_c$$

$$y'(0) = 0$$

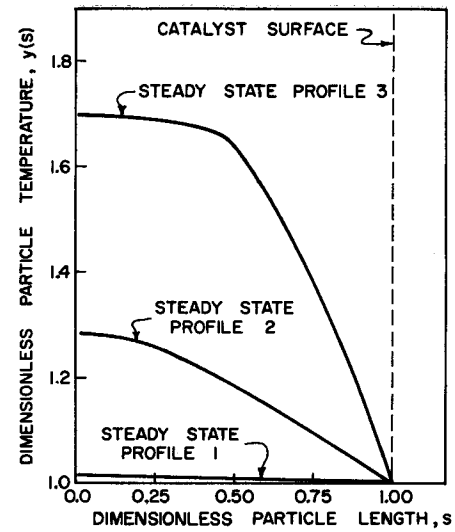

Fig. 18. Three steady state temperature profiles for Problem 2, Model 3.

This is a considerably easier system to solve, and the numerical solution tends to be stable by the Runge-Kutta-Gill routine used in this work. A consistency check on the computations is available since $y(1) = 1$, necessarily.

Five examples will be presented, the data for which are presented in Table 2.

Example 1: This is a case in which there is no maximum in the heat generation function as shown in Figure 11. y_L occurs at 1.04167, and the $S(y_c)$ curve is given in Figure 12 showing that only one steady state exists. The partial pressure and temperature profiles are given in Figure 13. Transient calculations starting from an initial perturbation are shown in Figure 14 showing that the steady state is approached. Figure 15 is a phase space plot showing the transient response surface from a start-up condition, $y = 1.000$, $z = 000$, for all x. The surface is swept out by curves (1), (2), (3), (4), (5) and the steady state profile.

Example 2: This example is one in which the heat generation function has a pronounced hump as shown in Figure 16. Figure 17 shows that there are three steady states at $y_c = 1.013$, 1.287, and 1.699, and Figure 18 shows the three possible temperature profiles. Transient calculations carried out with initial perturbations on temperature and partial pressure show that the intermediate

Table 2. Data and Results for Model 3

	Problem 1	Problem 2	Problem 3	Problem 4	Problem 5
$-\Delta H$	5,000	52,500	5,000	50,000	50,000
T_o	800	500	500	500	500
p_o	10.0	5.0	10.0	5.0	5.0
q	13.164	20.00	17.50	20.00	20.00
k'	10^{-5}	10^{-5}	9.375×10^{-5}	10^{-7}	4×10^{-5}
l	0.10	0.50	0.10	0.50	0.50
$\rho_s S_g$	10^6	2×10^6	2×10^6	2×10^6	2×10^6
γ	0.40	0.35	0.40	0.35	0.35
ρ_s	1.2	1.3	1.25	1.3	1.3
c_s	0.30	0.25	0.20	0.25	0.25
D	2×10^{-7}	4×10^{-7}	6×10^{-7}	4×10^{-7}	4×10^{-7}
$\lambda(1-\gamma)$	3×10^{-4}	3×10^{-4}	3×10^{-4}	3×10^{-4}	3×10^{-4}
Possibility of multiple states	no	yes	no	yes	yes
No steady states	one	three	one	one	one

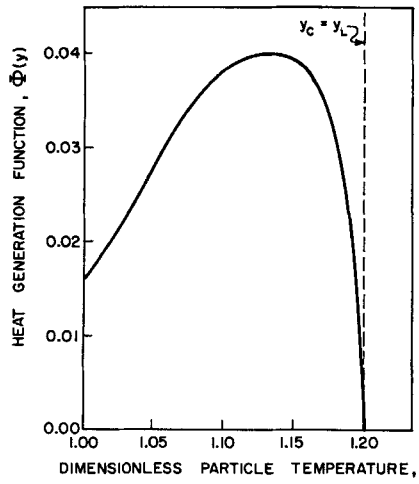

Fig. 19. Heat generation curve for Problem 3, Model 3.

state is unstable while the two outer states are stable. Corresponding graphs could be presented, but they appear no differently than others shown in this paper.

Example 3: This example is presented to illustrate the fact that although the heat generation function has a maximum, the curve of $S(y_c)$ vs. y_c is monotonically increasing and only one state can exist. Transient calculations show it to be stable. Figures 19 and 20 present the relevant curves. The profiles and transient curves present no new features.

Example 4: This is an example (no curves will be given) in which the heat generation function has a maximum and the possibility of steady states exists, but there is only one intersection of the $S(y_c)$ curve with $S(y_c) = 1$ and the state is stable by calculation.

Example 5: This example is similar to Example 4 except that there is a single intersection of $S(y_c)$ with $S(y_c) = 1$ at a high temperature in spite of the fact that there could be three intersections. The state is stable.

NOTATION

A = constant defined in Model 3
B = constant defined in Model 3

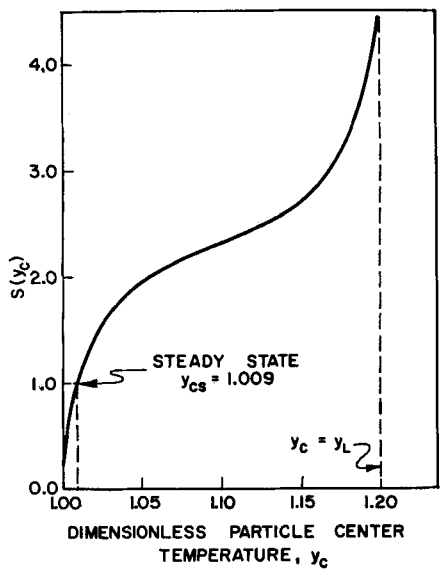

Fig. 20. $S(y_c)$ curve for Problem 3, Model 3.

b = constant defined in text
c_s = heat capacity of catalyst particle
c_{11}, c_{12}, c_{21}, c_{22} = constants defined in text for linearized problem
D = diffusivity
E = activation energy
h = heat transfer coefficient
H = dimensionless heat transfer coefficient
ΔH = heat of reaction $A \rightarrow B$
k = c_{11} c_{22} a constant
k' = frequency factor in reaction velocity constant
k_g = mass transfer coefficient
l = semiparticle thickness
M = constant defined in text
p = partial pressure of A in $A \rightarrow B$
p_o = surface partial pressure of A
P_s = steady state partial pressure
q = E/Rt_o
r = dimensionless space variable
R = gas constant
s = Laplace transform parameter
S_g = surface area of catalyst per gram of catalyst
t = temperature
t_o = surface temperature
t_s = steady state temperature
t_i = initial temperature
U = Laplace transform of dimensionless partial pressure perturbation
u = dimensionless partial pressure
u_i = initial dimensionless partial pressure
u_s = dimensionless steady state partial pressure
v = dimensionless temperature
v_i = dimensionless initial temperature
v_s = dimensionless steady state temperature
v_{sc} = dimensionless steady state center temperature
V = Laplace transform of dimensionless temperature perturbation
y = dimensionless temperature
y_c = dimensionless center temperature
y_L = dimensionless limiting temperature
z = dimensionless partial pressure

Greek Letters

α = constant defined in text
β = constant defined in text
γ_v = fraction void in particle
Δ = constant defined in text
ξ = dimensionless partial pressure perturbation
ξ_i = dimensionless initial partial pressure
η = dimensionless temperature perturbation
η_i = dimensionless initial temperature
ω = constant defined in text
ρ_s = catalyst density
θ = time
μ = constant defined in text
λ = thermal conductivity
γ = $\sqrt{\Delta^2 + s}$
τ = dimensionless time
σ = γ_v/Rt

LITERATURE CITED

1. Cannon, J., and K. G. Denbigh, *Chem. Eng. Sci.*, **6**, 155 (1957).
2. Copson, E. T., "Theory of Functions of a Complex Variable," Oxford University Press, England (1935).
3. Liu, Shean-lin, and Neal R. Amundson, *Ind. Eng. Chem. Fund.*, **1**, 200 (1962).
4. Wagner, C., *Chem.-Tech.*, **18**, 28 (1945).

Manuscript received July 31, 1964; revision received October 7, 1964; paper accepted October 8, 1964.